



Analysis of the long-term evolution of the solar resource in China and its main contributors

Chao Liu, Christophe Vernay, Lucien Wald, Philippe Blanc, Sébastien Pitaval

► To cite this version:

Chao Liu, Christophe Vernay, Lucien Wald, Philippe Blanc, Sébastien Pitaval. Analysis of the long-term evolution of the solar resource in China and its main contributors. SHC 2015, International Conference on Solar Heating and Cooling for Buildings and Industry, Dec 2015, Istanbul, Turkey. pp.1041-1052, 10.1016/j.egypro.2016.06.273 . hal-01353950

HAL Id: hal-01353950

<https://minesparis-psl.hal.science/hal-01353950>

Submitted on 16 Aug 2016

HAL is a multi-disciplinary open access archive for the deposit and dissemination of scientific research documents, whether they are published or not. The documents may come from teaching and research institutions in France or abroad, or from public or private research centers.

L'archive ouverte pluridisciplinaire **HAL**, est destinée au dépôt et à la diffusion de documents scientifiques de niveau recherche, publiés ou non, émanant des établissements d'enseignement et de recherche français ou étrangers, des laboratoires publics ou privés.

SHC 2015, International Conference on Solar Heating and Cooling for Buildings and Industry

Analysis of the long-term evolution of the solar resource in China and its main contributors

Chao Liu^a, Christophe Vernay^{b,*}, Lucien Wald^c, Philippe Blanc^c, Sébastien Pitaval^d

^a HUST University / Icare / Ecole Polytechnique, 1037 Luoyu Road, Wuhan, China

^b SOLAÏS, 400 avenue Roumanille, 06 906 Sophia Antipolis Cedex, France

^c MINES ParisTech – O.I.E. – Centre for Observation, Impacts, Energy, CS 10207, 06 904 Sophia Antipolis Cedex, France

^d THIRD STEP, No.580 West Nanjing Road, Shanghai, China

Abstract

This work analyses the long-term trend of the daily global (GHI) and diffuse (DHI) irradiances received on a horizontal plane for four cities in China: Harbin, Beijing, Wuhan and Guangzhou, located from North to South. Measurements of GHI and DHI between 1990 and 2013 have been retrieved from GEBA and WRDC networks. During this period, the yearly mean of the GHI increases for most of the sites (0.1 to 0.7% per year) except for Harbin for which it decreases (-0.4% per year) while the yearly mean of the DHI increases for all sites (0.2 to 0.9% per year). The effects of the aerosol optical depth at 550 nm and the cloud cover on such changes have been investigated. It has been found that aerosols have a direct impact on GHI in clear-sky conditions, especially for Beijing and Wuhan, and that the correlation is strong between the GHI measurements for all-sky conditions and aerosol optical depth at 550 nm. Expectedly, the correlation is much more significant between the GHI measurements and the cloud cover.

© 2016 The Authors. Published by Elsevier Ltd. This is an open access article under the CC BY-NC-ND license (<http://creativecommons.org/licenses/by-nc-nd/4.0/>).

Peer-review by the scientific conference committee of SHC 2015 under responsibility of PSE AG

Keywords: global and diffuse horizontal irradiation; aerosol; cloud cover; ground-based measurement; China.

* Corresponding author. Tel.: +33 (0)4 83 88 02 93; fax: +33 (0)4 93 00 88 14.
E-mail address: cvernay@solais.fr

1. Introduction

China is currently a huge commercial market for the solar industry, from photovoltaics (PV) to solar heating systems. Its vast territory spans from approximately 18° N to 55° N, i.e. mid- and low latitudes with a large potential in solar resource. Air quality in large cities in China is often low; these levels of air pollution must be taken into consideration and the evolution of the daily global irradiation on horizontal surface (GHI) on several decades must be studied in order to gain confidence in economic models of future projects.

This paper presents the analysis of long-term ground-based measurements of GHI for several sites in China and to investigate the causes of the changes with time.

Nomenclature and variables

AOD	aerosol optical depth
ASL	above sea level
BSRN	Baseline Surface Radiation Network
CRU	Climate Research Unit, University of East Anglia
DHI	daily diffuse irradiation received on a horizontal plane
GEBA	Global Energy Balance Archive
GHI	daily global irradiation received on a horizontal plane
TOA	top of atmosphere
WRDC	World Radiation Data Centre

C	monthly cloud cover from CRU
G, D	GHI, DHI
$G_{\text{clear}}, D_{\text{clear}}$	GHI, DHI in clear-sky conditions
$G_{\text{GE}}, D_{\text{GE}}$	GHI, DHI from the GEBA database
$G_{\text{GR}}, D_{\text{GR}}$	GHI, DHI measured by ground-based stations
$G_{\text{WR}}, D_{\text{WR}}$	GHI, DHI from the WRDC database
$E0$	GHI on top of atmosphere
KT	daily clearness index
τ_{550}, τ_{1240}	daily AOD at 550 nm, respectively 1240 nm

Subscripts m , respectively y mean ‘monthly’ and ‘yearly’

2. Measurements and stations

China has a vast territory covered by a large number of measuring stations. This study uses measurements that are available through international networks: GEBA and WRDC.

2.1. GEBA and WRDC networks

The Global Energy Balance Archive (GEBA) is a database which contains monthly means of surface solar irradiance from 1500 ground-based meteorological stations [1]. Suspicious data are flagged by quality assessment procedures performed prior to their inclusion in the database. By taking into account the number of hours and days in a month, monthly or yearly means of GHI or DHI (diffuse irradiation) can be computed.

Data on GHI during the period 1988-2013 are available from World Radiation Data Centre (WRDC, <http://wrdc.mgo.rssi.ru/>). WRDC built a database of GHI and DHI by collecting data from national weather services under the World Meteorological Organization (WMO). There are 8 WRDC stations available in China with quality flags.

2.2. Selection of representative sites

Table 1 depicts the four main sites in China that have been studied in the present study, using a North-to-South sorting. Several terms were considered in the selection process. Firstly, the four sites span from North to South and reflect the main features of the GHI in China. Secondly, a ground-based station is available for each selected location, belonging to both GEBA and WRDC networks, thus allowing the cross-validation of data. Thirdly, data on GHI and DHI are available for the four sites during the period 1990-2013. The four sites are scattered throughout China and are deemed to represent the climate for their specific regions.

Table 1. Information of the four selected sites

Sites	GEBA name	WRDC name	Latitude (°)	Longitude (°)	Elevation (<i>m</i> asl)
Harbin	GEBA2039 Harbin	WRDC Harbin	45.750	126.767	142
Beijing	GEBA2042 Beijing	WRDC Beijing	39.800	116.467	32
Wuhan	GEBA2046 Wuhan	WRDC Wuhan	30.617	114.133	23
Guangzhou	GEBA2048 Guangzhou	WRDC Guangzhou	23.167	113.333	41

2.3. Clearness index

Let note $E0$ the daily irradiation received on a horizontal plane at the top of atmosphere (TOA). It is directly linked to latitude: the closer to the equator, the greater $E0$. If G_m denotes the monthly mean of the GHI, the monthly clearness index KT_m is defined as:

$$KT_m = G_m / (E0)_m \quad (1)$$

KT gives the percentage of the irradiation which reaches the ground from the top of atmosphere. By using KT , three categories of sky conditions have been defined:

- overcast: $KT \leq 0.3$
- intermediate: $0.3 < KT \leq 0.7$
- clear-sky (cloud-free): $0.7 < KT$

2.4. Quality check (QC)

GEBA and WRDC database have their own quality assessment (QA) with flags on the measurements in order to remove suspicious data. An additional quality check (QC) is performed on each data set with the following constraints [3]:

- $333 \text{ Wh m}^{-2} < G < 0.9 * E0$
- $D \leq G$

Table 2 exhibits the results of QC for both monthly data from GEBA and daily data from WRDC for the four sites. GEBA and WRDC have respectively 252 monthly and 8766 daily measurements for GHI or DHI. 0.4% to 6.6% of the monthly data of GEBA are flagged out over QA and up to 0.4% over QC. Among the four sites, Wuhan has the greatest number of flagged values: 6.6% over QA, while there are no flag for Guangzhou over QA and Beijing, Wuhan, and Guangzhou over QC. For WRDC, there are 1.2% to 7.7% of the daily data flagged out for the four sites over QA and 0.5% to 2.0% over QC. Among the four sites, Wuhan has the greatest number of flagged values: 7.7% over QA, while there are 0.5% and 0.6% values flagged for Harbin and Beijing over QA.

The percentage of data filtered by the QC for the four sites is low: 0.1% (GEBA) and 1.0% (WRDC). It is much less than that of the data flagged by the QA: 2.3% (GEBA) and 3.6% (WRDC). This may be explained by the high quality of the QA performed by GEBA and WRDC and by the low constraints in QC. It can be assumed that the data filtered by QA and QC are reliable for the study.

Table 2. Quality checks for concatenated GHI and DHI monthly data between 1990 and 2010 (GEBA) and daily data between 1990 and 2013 (WRDC).

	GEBA 1990-2010				WRDC 1990-2013			
	Number of data	% QA	% QC	Final number of data	Number of data	% QA	% QC	Final number of data
Harbin	504	0.4%	0.4%	500	17532	1.2%	0.5%	17249
Beijing	504	2.2%	0	493	17532	3.4%	0.6%	16832
Wuhan	504	6.6%	0	471	17532	7.7%	2.0%	15864
Guangzhou	504	0	0	504	17532	2.3%	1.1%	16947
Total	2016	2.3%	0.1%	1968	70128	3.6%	1.0%	66892

3. Analysis of the irradiation estimated in clear-sky conditions

3.1. The McClear clear-sky model

McCclear is a new clear-sky model which estimates GHI and DHI at ground level under clear-sky conditions [4]. It is available as a web service through the SoDa Service (www.soda-pro.com) and delivers time series of irradiation G_{clear} and D_{clear} . Inputs to McCclear include aerosol properties through aerosol optical depth (AOD), total column content in water vapour, and ozone provided by the EU-funded MACC project (Monitoring Atmosphere Composition and Climate). The AOD is provided for two wavelengths: 550 and 1240 nm, denoted by τ_{550} and τ_{1240} . Partial AODs at 550 nm are given for black carbon (BC), dust (DU), particulate organic matter (POM), sea salt (SS) and sulfate (SU). They help in depicting the influence of human activities on the irradiation at ground level. The data of GHI and DHI from McCclear in China during 2004-2014 has been collected.

McCclear has been accurately validated in the BSRN station of Xianghe in China, close to Beijing [4]. It has been observed that McCclear is providing accurate estimates of the global and diffuse irradiation for Xianghe. This high accuracy of McCclear is also found for other stations all over the world [4]. Therefore, it is assumed that estimates provided by McCclear are accurate to other locations in China, and especially to the four selected sites.

3.2. McCclear analysis for the four sites

Fig. 1 depicts the evolution of both $(G_{\text{clear}})_y$ and $(\tau_{550})_y$, with respect to their long-term average, between 2004 and 2014 for the four sites. Fig. 1a demonstrates that the irradiation in 2014 is lower than the one in 2004. Least square fitting reveals a systematic decrease of $(G_{\text{clear}})_y$ over the period 2004-2014, with a greater decrease in the North of China. $(G_{\text{clear}})_y$ decreases more in Harbin and Beijing than in the two other sites and Beijing decreases most. For Guangzhou, there is a positive trend with time for $(G_{\text{clear}})_y$ until 2012 and then a sudden decrease in 2013 and 2014. $(KT_{\text{clear}})_y$ is in the range of 0.58 (Wuhan) to 0.66 (Harbin), and values in Beijing and Wuhan are quite less than those in Harbin and Guangzhou (Table 3).

From Fig. 1b, $(\tau_{550})_y$ ranges from 0.35 (Harbin) to 0.73 (Wuhan). There are positive trends with time for $(\tau_{550})_y$ in Harbin and Beijing and negative trends in Wuhan and Guangzhou. $(\tau_{550})_y$ increases the most in Beijing with more than 20% from 2004 to 2014, while $(\tau_{550})_y$ declines the most in Guangzhou with more than 10% during the same period.

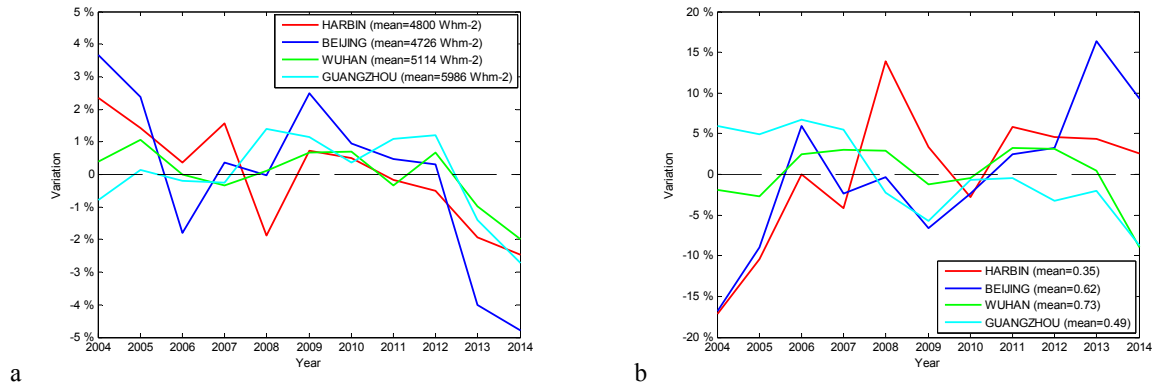


Fig. 1. (a) Variation of a) $(G_{\text{clear}})_y$ and b) $(\tau_{550})_y$ with respect to their long term average from 2004 to 2014.

Table 3. Variation of $(G_{\text{clear}})_y$ from 2004 to 2014.

Sites	Mean $(G_{\text{clear}})_y$ (Wh m^{-2})	Total variation	Variation per year	Mean $(E0)_y$ (Wh m^{-2})	$(KT_{\text{clear}})_y$
Harbin	4800	-4.2%	-0.4%	7318	0.66
Beijing	4726	-6.1%	-0.6%	7933	0.60
Wuhan	5114	-1.8%	-0.2%	8754	0.58
Guangzhou	5986	-1.0%	-0.1%	9284	0.64

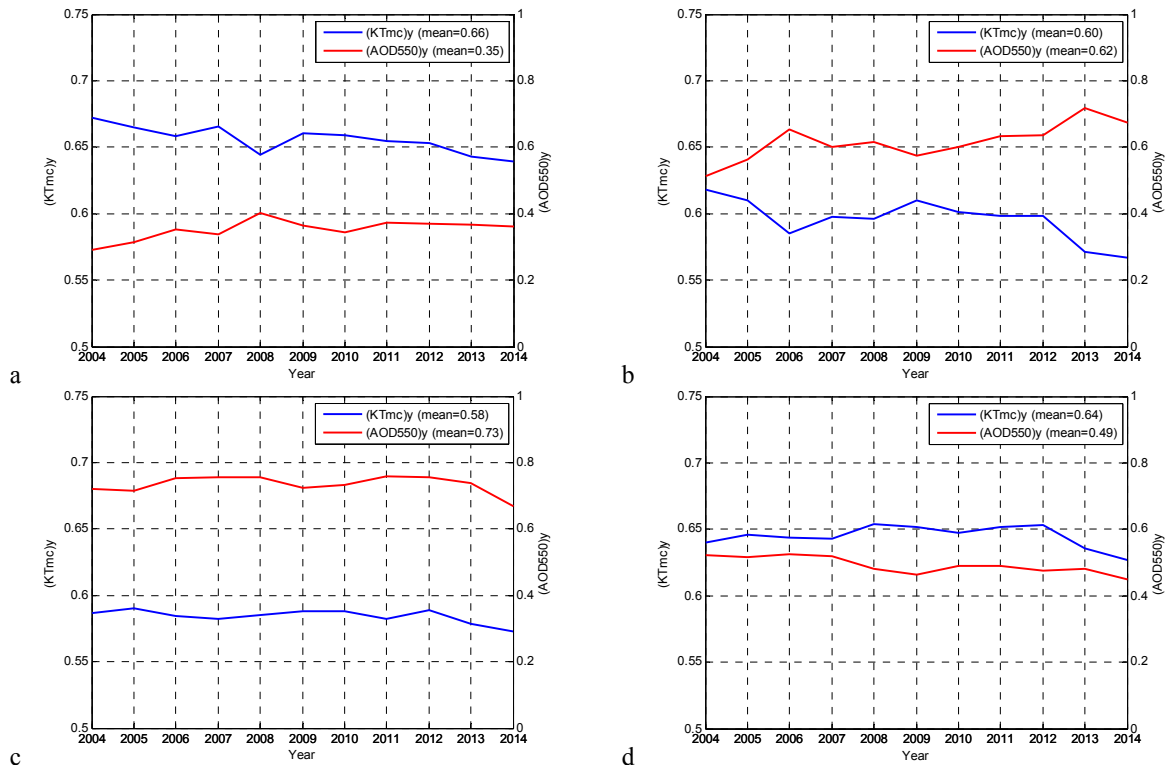
As introduced previously, estimates of the irradiation at surface under clear-sky conditions partly provide indications on the effect of human activities on the irradiation level. Regarding $(G_{\text{clear}})_y$, Beijing has the lowest value and Guangzhou the greatest. The high correlation between τ_{550} and KT_{clear} , especially for Beijing and Wuhan, shows the direct link between the aerosols and G_{clear} . However, Guangzhou has a downward trend for $(\tau_{550})_y$, whereas it increases in both Beijing and Harbin (most in Beijing). That explains why $(G_{\text{clear}})_y$ declines the most for Beijing. On the short term, $(G_{\text{clear}})_y$ is more likely to continue to decrease less in Wuhan and Guangzhou than those in Harbin and Beijing.

3.3. Analysis of $(\tau_{550})_y$ and $(KT_{\text{clear}})_y$

Table 4 shows that KT_{clear} and consequently G_{clear} have greater correlations with τ_{550} than with τ_{1240} in the four sites. τ_{550} is also available for the five following species: black carbon (BC), dust (DU), particulate organic matter (POM), sea salt (SS) and sulfate (SU). Black carbon and sulfate show greater correlations with KT_{clear} than others and sea salt has the lowest correlations. From Fig. 2, it can be seen that high means of $(\tau_{550})_y$ relate to low means of $(KT_{\text{clear}})_y$ for the four sites. It is expected that a decrease of $(\tau_{550})_y$ from one year to another should lead to an increase of $(KT_{\text{clear}})_y$. This is well observed in the four sites for the whole period with a few exceptions: transition 2009-2010, 2011-2012, 2013-2014 in Harbin, 2013-2014 in Beijing, 2012-2013, 2013-2014 in Wuhan and 2008-2009, 2013-2014 in Guangzhou. One can observe that the magnitude of year-to-year change in $(\tau_{550})_y$ does not always yield the same magnitude of change in $(KT_{\text{clear}})_y$.

Table 4. Correlation coefficient on KT_{clear} versus τ_{550} , τ_{1240} , and τ_{550} for five species: BC, DU, POM, SS and SU.

	τ_{550}	τ_{1240}	BC	DU	POM	SS	SU
Harbin	-0.76	-0.73	-0.66	-0.58	-0.41	-0.39	-0.72
Beijing	-0.81	-0.68	-0.80	-0.47	-0.68	-0.44	-0.76
Wuhan	-0.77	-0.66	-0.77	-0.29	-0.49	-0.03	-0.76
Guangzhou	-0.84	-0.77	-0.81	-0.48	-0.67	-0.08	-0.80

Fig. 2. $(KT_{\text{clear}})_y$ from McClear, in blue, and $(\tau_{550})_y$ from MACC, in red, from 2004 to 2014: (a) Harbin; (b) Beijing; (c) Wuhan; (d) Guangzhou

It can be concluded that τ_{550} had a heavy impact on G_{clear} during 2004–2014 and it should present the same trend in the future. The correlation is great between KT_{clear} and τ_{550} , so studying the variations of τ_{550} brings valuable information.

4. Measurements (GEBA and WRDC)

4.1. Deviation between GEBA and WRDC

For each of the four sites, data of WRDC and GEBA originate from the same ground-based station source and should be similar. 2D histograms with GEBA (x-axis) and WRDC (y-axis) have been drawn in Fig. 3 to verify this similarity. Following the ISO standard [6], the deviations were computed by subtracting the GEBA measurements from the WRDC ones. Expectedly, most observations lie around the 1:1 line in each graph. Beijing presents the greatest similarity between WRDC and GEBA. Harbin presents the same trend but with some abnormal points. For Wuhan and Guangzhou, values from WRDC are slightly greater than those from GEBA. Table 5 gives a detailed

comparison of the monthly sum of GHI for GEBA and WRDC. Three statistical measures are computed: the correlation coefficient and the bias and standard deviation relative to the mean observed value which is GEBA for these figures. Relative values are expressed with respect to. The results show that the relative bias and standard deviation for the four sites range between 0.3 and 3.8% and that the correlation coefficients are greater than 0.996.

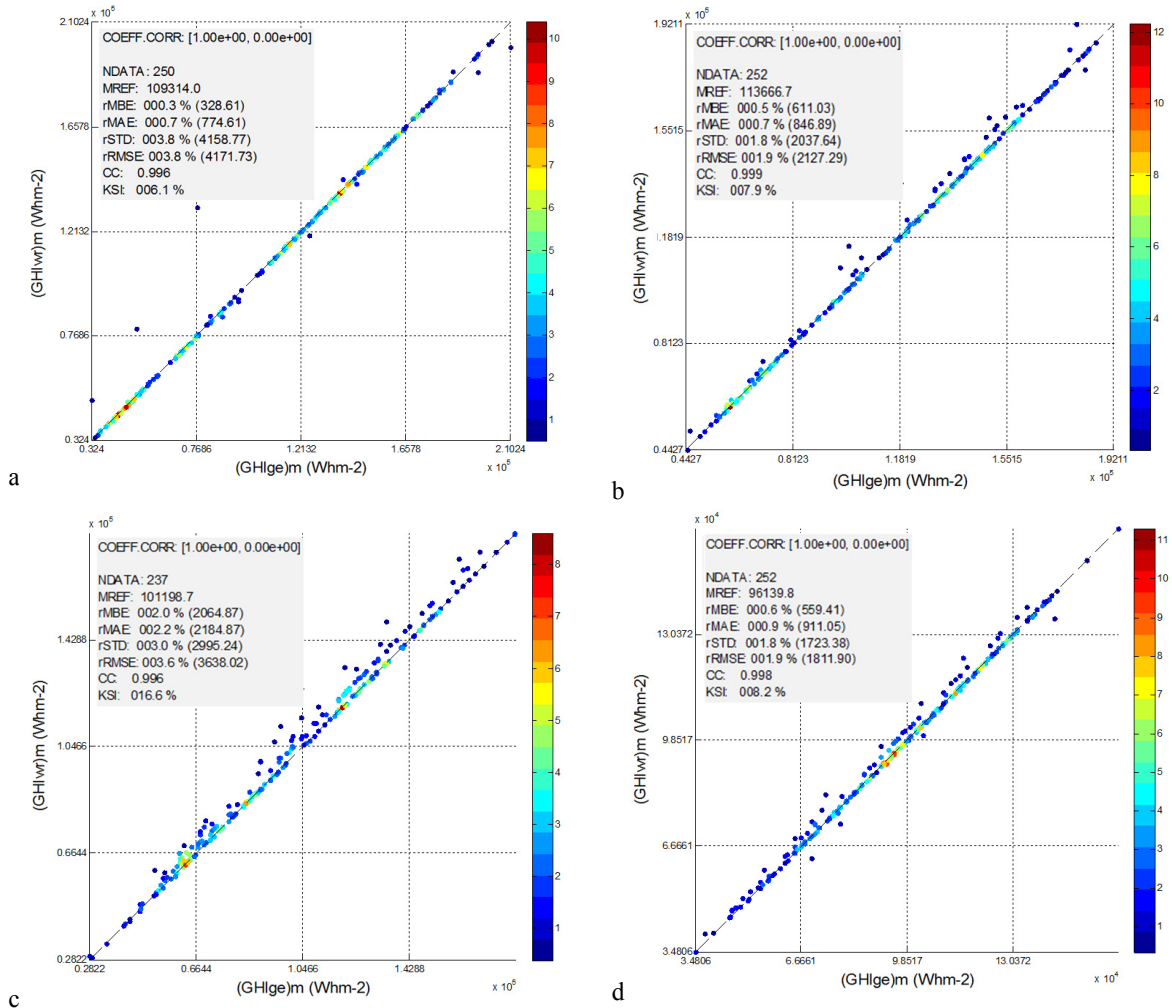


Fig. 3. 2D histograms between GEBA (X-axis) and WRDC (Y-axis) for the monthly sum of GHI during 1990-2010: (a) Harbin; (b) Beijing; (c) Wuhan; (d) Guangzhou.

It is concluded that the WRDC data sets exhibit high quality enough so that the data from 2011-2013 can be added to the GEBA data sets in order to extend the analysis period up to 2013. Hence, all data are concatenated when possible, i.e. on a monthly or yearly basis. These consolidated new data sets are called G_{GR} and D_{GR} . Finally, yearly means of daily irradiation over the period 1990-2013 are constructed using these ground measurements, so called $(G_{GR})_y$ and $(D_{GR})_y$.

Table 5. Comparison of the monthly sum of GHI from between GEBA and WRDC for the period 1990 to 2010; GEBA data is the reference.

Sites	Number of data	Relative bias	Relative standard deviation	Correlation coefficient
Harbin	250	0.3%	3.8%	0.996
Beijing	252	0.5%	1.8%	0.999
Wuhan	237	2.0%	3.0%	0.996
Guangzhou	252	0.6%	1.8%	0.998

4.2. GHI and DHI measurements

As shown in Fig. 4, from 1990 to 2013, $(G_{GR})_y$ decreases slightly in Harbin and increases slightly in Beijing, while Wuhan and Guangzhou showed apparent positive trends with time. Table 6 gives variations of $(G_{GR})_y$ and $(D_{GR})_y$ during the period. The mean value of $(G_{GR})_y$ is the greatest in Beijing (3700 Wh m^{-2}), and the lowest in Guangzhou (3200 Wh m^{-2}), which does not reflect the trend of the irradiation when considering latitude only. The mean of $(D_{GR})_y$ is in the range of $1600\text{--}2000 \text{ Wh m}^{-2}$ for the four sites. $(G_{GR})_y$ and $(D_{GR})_y$ in Wuhan and Guangzhou increase much more with time than in Harbin and Beijing. Except $(G_{GR})_y$ in Harbin, $(G_{GR})_y$ and $(D_{GR})_y$ both present upward trends during 1990–2013.

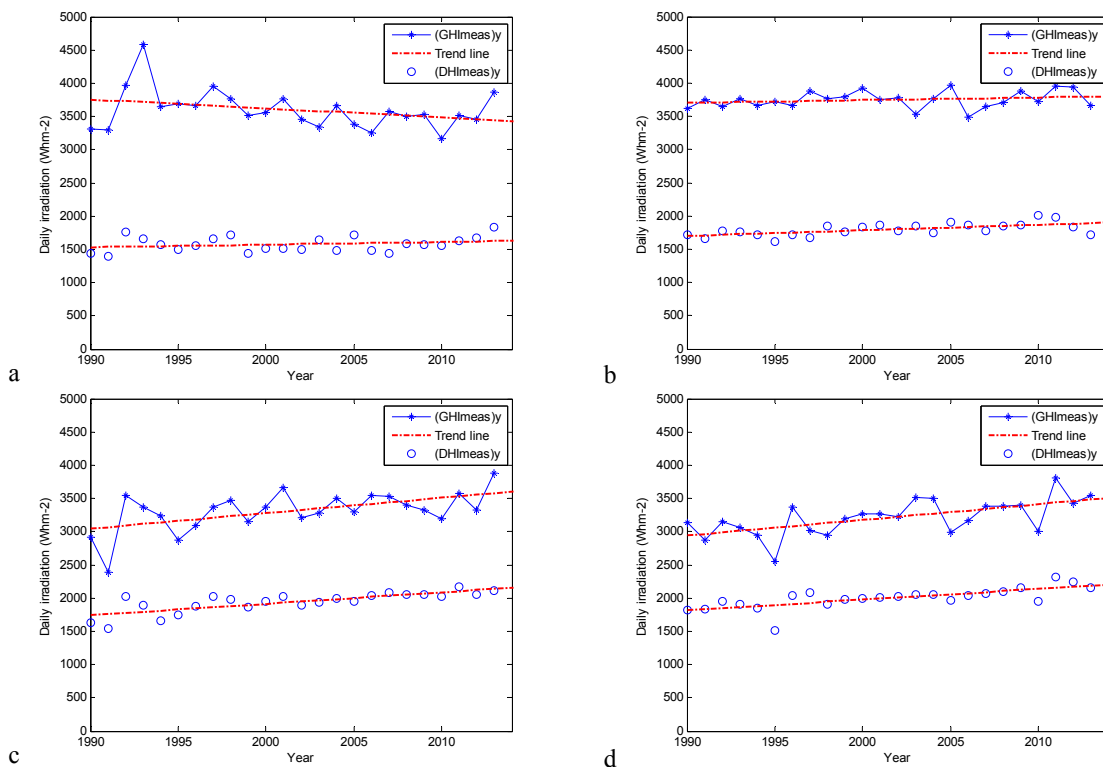


Fig. 4. Consolidated $(G_{GR})_y$ and $(D_{GR})_y$ during 1990–2013: (a) Harbin; (b) Beijing; (c) Wuhan; (d) Guangzhou

Table 6. Variation of $(G_{GR})_y$ and $(D_{GR})_y$ during 1990-2013.

Sites	Mean $(G_{GR})_y$ (Wh m ⁻²)	Total variation	Variation per year	Mean $(D_{GR})_y$ (Wh m ⁻²)	Total variation	Variation per year
Harbin	3601	-8.7%	-0.4%	1578	5.9%	0.2%
Beijing	3749	2.6%	0.1%	1798	10.7%	0.4%
Wuhan	3314	16.7%	0.7%	1941	21.0%	0.9%
Guangzhou	3213	17.2%	0.7%	2001	19.2%	0.8%

After comparing Fig. 4 with Fig. 1, the same evolution from one year to the other between $(G_{GR})_y$ and $(G_{clear})_y$ in Harbin and Beijing are well observed from 2004 to 2013 with a few exceptions: 2010-2011, 2012-2013 in Harbin and 2004-2005, 2007-2008, 2010-2011 in Beijing. But for the two other sites, only 2006-2007 in Wuhan and 2009-2010, 2010-2011 in Guangzhou show the same trends. It can be seen in Table 7 that the correlation between G_{clear} and G_{WR} declines from Harbin to Guangzhou. It is apparent that there is a high agreement between G_{clear} and G_{WR} in Harbin and Beijing. It demonstrates that the cloud cover impacts more GHI in Guangzhou than in the other three sites. The deviation in correlation coefficient for the four sites is related to changes in cloud cover; this point is discussed later.

Table 7. Correlation coefficient between G_{clear} and G_{WR} .

Correlation coefficient	
Harbin	0.81
Beijing	0.79
Wuhan	0.61
Guangzhou	0.29

The analysis of $(G_{GR})_y$ and $(D_{GR})_y$ shows upward trends from 1990 to 2013 in the four sites, except $(G_{GR})_y$ in Harbin, as shown in Table 6. $(G_{GR})_y$ and $(D_{GR})_y$ in Wuhan and Guangzhou, located in the South of China, increased much more than in Harbin and Beijing, located in the North of China. Changes of $(G_{GR})_y$ do not correspond directly to changes in $(D_{GR})_y$ so that changes in cloud cover can partly explain such changes.

4.3. Comparing $(G_{GR})_m$ and $(G_{clear})_m$

$(G_{GR})_m$ for the period 1990-2013 is compared with $(G_{clear})_m$ for the period 2004-2014 for which estimates of clear-sky radiation by McClear are available. Fig. 5 exhibits the maximum and minimum values for $(G_{GR})_m$ for the four sites while the deviation between $(G_{GR})_m$ and $(G_{clear})_m$ originates from the effects of cloud. The deviation between $(G_{GR})_m$ and $(G_{clear})_m$ in Guangzhou is much greater than those in Wuhan, and then Beijing and Harbin.

It demonstrates that cloud cover contributes to the deviations. The overestimation from McClear in Guangzhou is deemed as a result of more cloud cover in Guangzhou as shown in Fig. 5. The difference between $(G_{GR})_m$ and $(G_{clear})_m$ increases from Harbin to Guangzhou. The cloud cover contributes to this difference, so when G_{clear} is used to evaluate solar resource in a specific area, cloud cover should be considered.

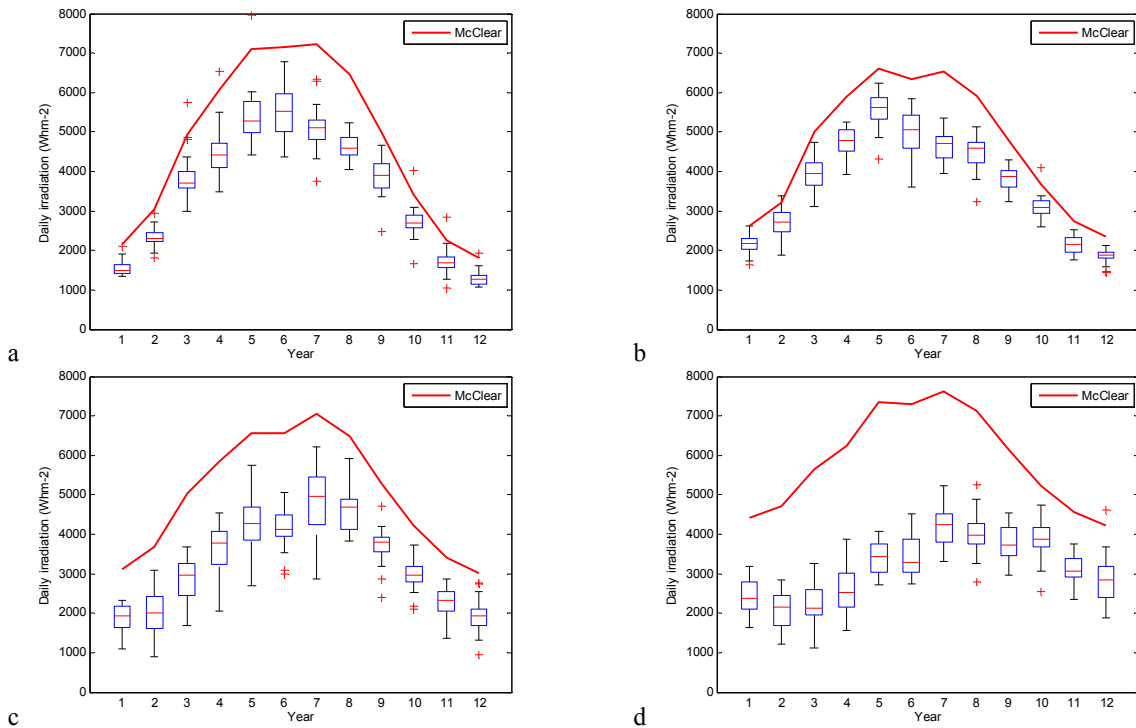


Fig. 5. Boxplots of $(G_{GR})_m$ during 1990-2013 and average curve of $(G_{clear})_m$ during 2004-2014: (a) Harbin; (b) Beijing; (c) Wuhan; (d) Guangzhou

4.4. Cloud cover

The cloud cover (also known as cloudiness) is an important factor for the irradiation. Monthly cloud cover (C) information for the four sites has been retrieved on the 2001-2010 period from the monthly data set provided by the Climate Research Unit of the University of East Anglia [6]. Fig. 6 exhibits the variation of $(C)_y$ for the four sites from 2001 to 2010. Mean $(C)_y$ in Harbin has the lowest value (35.3%) while Guangzhou has the highest (69.3%). Except Harbin, $(C)_y$ in other three sites shows slight increases during the period. Least square fitting shows systematic increases for the four sites over the whole period and $(C)_y$ in Guangzhou increases most. It can be concluded that cloud cover reduces GHI in the four sites during from 2001 to 2010. An increase of $(C)_y$ with a decrease of $(G_{GR})_y$ is also observed between Fig. 6 and Fig. 4 on the period 2001-2010.

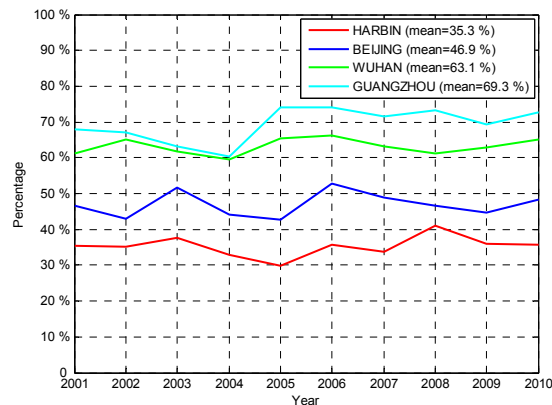


Fig. 6. $(C)_y$ from 2001 to 2010 for the four sites: Harbin, Beijing, Wuhan and Guangzhou

4.5. Analysis of $(C)_y$, $(KT_{GE})_y$ and $(\tau_{550})_y$

Fig. 7 exhibits variations on $(C)_y$, $(KT_{GE})_y$ and $(\tau_{550})_y$ from 2001 to 2010 in the four sites. A decrease of cloud cover leads to an increase of $(KT_{GE})_y$ in Beijing. The consistency in Beijing is more noticeable than those in Harbin, Wuhan and Guangzhou, but these three sites also have good correlations between $(C)_y$ and $(KT_{GE})_y$. In Beijing, $(\tau_{550})_y$ and $(KT_{GE})_y$ also show opposite trends during 2004-2010 except for 2004-2005 and 2007-2008 transitions. This illustrates that cloud cover has a greater impact on the irradiation than τ_{550} .

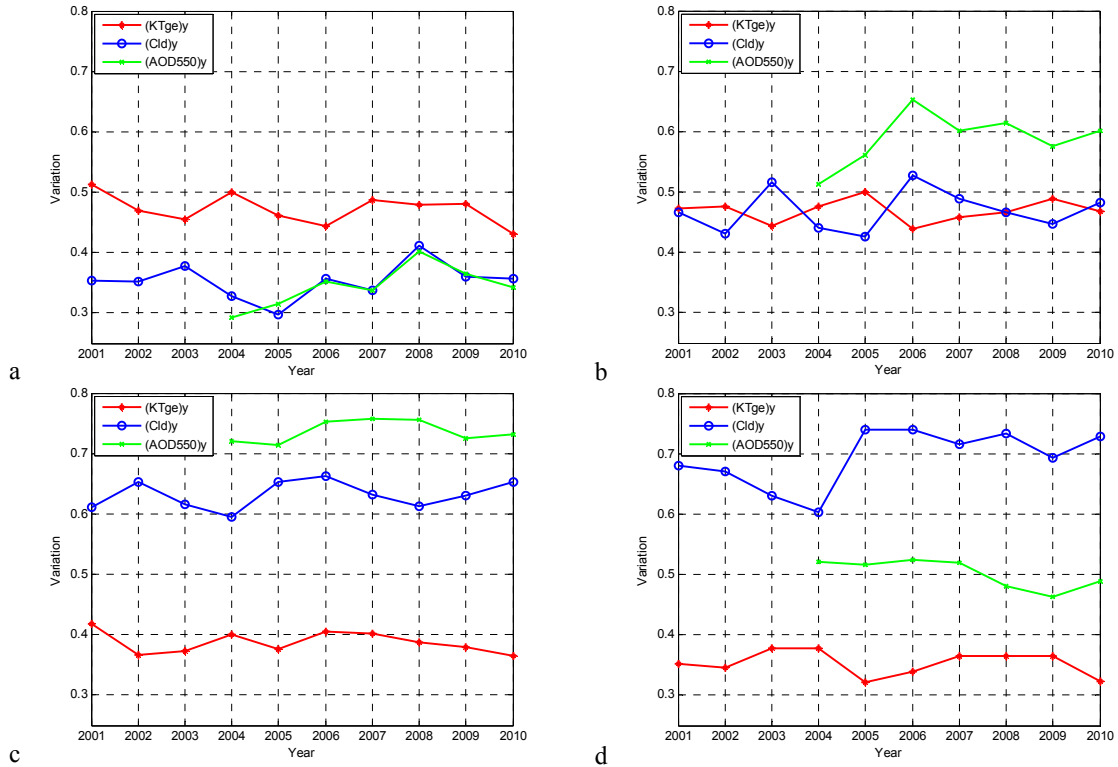


Fig. 7. $(KT_{GE})_y$, $(C)_y$ and $(\tau_{550})_y$ from 2001 to 2010: (a) Harbin; (b) Beijing; (c) Wuhan; (d) Guangzhou

Table 8 provides the correlation coefficient between $(C)_m$ and $(KT_{GE})_m$. Expectedly, it is negative for all sites illustrating the negative effect of the cloud cover on the GHI. Correlation coefficients are much smaller in Harbin (-0.12) and Wuhan (-0.43) than those in Beijing (-0.77) and Guangzhou (-0.82). It illustrates that besides cloud cover, there are still other factors like τ_{550} which impact the irradiation.

Table 8. Correlation coefficient between $(C)_m$ and $(KT_{GE})_m$
Correlation coefficient

Harbin	-0.12
Beijing	-0.77
Wuhan	-0.43
Guangzhou	-0.82

5. Conclusions

Four main sites in China have been selected for the present study, using a North-to-South sorting: Harbin, Beijing, Wuhan and Guangzhou for which GEBA and WRDC ground-based measurements are available. The long-term evolutions of the GHI and DHI have been analyzed through the processing of ground-based measurements of the irradiation and the cloud cover, along with the estimation of aerosol and clear-sky GHI.

$(G_{\text{clear}})_y$ systematically decreases between 2004-2014 for the four sites. G_{clear} provides some indications on the effect of human activities on the irradiation and G_{clear} in the four sites have high correlations with τ_{550} . Regarding the mean $(G_{\text{clear}})_y$, Beijing has the lowest value and Guangzhou the highest. In next few years, $(G_{\text{clear}})_y$ is more likely to continue to decrease in Harbin and Beijing while it may decrease less or increase in Wuhan and Guangzhou. There is good correlation between KT_{clear} and τ_{550} , supporting further work on changes in τ_{550} variation to better understand changes in G_{clear} .

One can observe positive trends with time of the measured G_{GR} and D_{GR} for the four sites, except G_{GR} in Harbin. The increase is more significant in Wuhan and Guangzhou than in Harbin and Beijing. Mean $(G_{\text{GR}})_y$ in ascending order for the four sites is Guangzhou, Wuhan, Harbin and Beijing. The order is not the same for G_{clear} and the cloud cover contributes to this discrepancy. In the next few years, G_{GR} will likely increase for the four sites, especially for Wuhan and Guangzhou. Cloud cover has a stronger impact on G_{GR} than τ_{550} .

The deviation between G_{GR} and G_{clear} increases southwards from Harbin, Beijing and Wuhan to Guangzhou. It is mostly due to the cloud cover; the cloud cover must also be considered when G_{clear} is used to evaluate the solar resource in a specific area. The cloud cover increases for the four sites from 2001 to 2010 while the measured GHI shows an opposite trend on the same period.

Except for G_{GR} in Harbin, both G_{GR} and D_{GR} present an positive trend from 1990 to 2013, especially for Wuhan and Guangzhou. This trend is negatively correlated with trends in cloud cover. However, the cloud cover cannot be the unique cause of the changes in solar radiation. Changes in τ_{550} play a role even though its contribution is less important than the cloud cover. [7] have observed that in 27 cities across China GHI and wind speed track similar decadal trends in 1961–2011, suggesting wind speed as a possible regulator of the GHI through interactions with aerosols.

Acknowledgements

The present works have been conducted thanks to the SoDa Service (www.soda-pro.com), the GEBA and WRDC networks, and the Climate Research Unit of the University of East Anglia which respectively provided time series of clear-sky irradiation and AOD, ground-based measurements and cloud cover data.

References

- [1] Gilgen H, Ohmura A. The Global Energy Balance Archive. Bulletin of the American Meteorological Society; 1999, 80, 831–850.
- [2] Ohmura A., Gilgen H., Hegner H., Mueller G., Wild M., Dutton E. G., Forgan B., Froelich C., Philipona R., Heimo A., Koenig-Langlo G., McArthur B., Pinker R., Whitlock C. H., and Dehne K. Baseline Surface Radiation Network (BSRN/WCRP): new precision radiometry for climate research, Bulletin of the American Meteorological Society, 1998; 79, 2115–2136.
- [3] Geiger M, Diabaté L, Ménard L, Wald L. A Web Service for controlling the quality of measurements of global solar irradiation. Solar Energy, 2002; 73, 475–480.
- [4] Lefevre M, Oumbe A, Blanc P, Espinar B, Gschwind B, Qu Z, Wald L., Schroedter-Homscheidt M., Hoyer-Klick C., Arola A., Benedetti A., Kaiser J. W., Morcrette J.-J. McClear: a new model estimating downwelling solar radiation at ground level in clear-sky conditions. Atmospheric Measurement Techniques, 2013, 6, 2403–2418.
- [5] ISO Guide to the Expression of Uncertainty in Measurement: first edition, International Organization for Standardization, Geneva, Switzerland, 1995.
- [6] New M, Hulme M, Jones P. Representing twentieth-century space-time climate variability. Part II: development of 1901–96 monthly grids of terrestrial surface climate. Journal of Climate, 2000, 13, 2217–2238.
- [7] Wang Y. W., Yang Y. H., Zhou X. Y., Zhao N., Zhang J. H. Air pollution is pushing wind speed into a regulator of surface solar irradiance in China. Environ. Res. Lett. 2014, 9 054004